Stochastic modeling of geometric imperfections for buckling analysis of suction buckets

Journal of Physics: Conference Series **2362** (2022) 012007 doi:10.1088/1742-6596/2362/1/012007

Stochastic modeling of geometric imperfections for buckling analysis of suction buckets

M Böhm, P Schaumann

Institute for Steel Construction, Leibniz University Hannover - ForWind, Appelstrasse 9, 30167 Hannover, Germany

E-mail: boehm@stahl.uni-hannover.de

Abstract. Recently, suction buckets have become a very prominent foundation for bottom fixed and floating offshore wind turbines. They are embedded with an installation force that stems from water evacuation inside the bucket. This internal negative pressure leads to a high risk of structural buckling. The buckling strength is significantly reduced by geometric imperfections. In previous work, equivalent geometric imperfection forms were introduced and the lower bound was evaluated. However, it has not yet been possible to identify a generally appropriate imperfection form. A probabilistic design approach based on realistic imperfections was not yet considered for suction buckets. Therefore, in this work, a stochastic modeling approach is introduced, which bases on measured data. The imperfection is decomposed to the half-wave cosine Fourier representation. Realizations of the imperfection pattern are generated by filtering white noise with the amplitude spectrum. They are then applied as out of plane deviations on a geometrically and materially nonlinear finite element model and evaluated. The resulting buckling pressure distribution can then be evaluated for different reliability levels. By considering more realistic imperfections and a plastic soil model, the buckling pressure increases by up to a factor of two compared to the conservative stress-based buckling approach.

1. Introduction

Suction buckets are large cylindrical shell structures used as foundations for offshore wind turbines. Due to the low noise emission during installation as well as the possibility of dismantling, they are considered as a promising environmentally friendly alternative to pile foundations of offshore wind turbines. Further, due to the low embedment depth, they are suitable for soil conditions, where monopiles cannot be installed. If design uncertainties can be minimized, it is likely that the steel demand will be significantly lower than for piles, which would then allow for a more economical and ecological structure. However, the installation process of suction buckets poses some challenges. A potential risk arises from the large amount of soil in contact with the structure, where high variability in soil properties, hard inclusions or boulders could be encountered. Further, the installation pressure differential depends significantly on the soil type and soil strength. This pressure differential creates a suction on the lid, which increases the downward force and also generates seepage in the soil, which reduces the skirt tip resistance. The minimum pressure to overcome the soil resistance is dependent on soil properties as well as the embedment depth and the maximum pressure is determined by hydraulic failure or piping. The applicable maximum installation pressure is further limited by structural buckling.

With increasing turbine size and water depth, the bucket dimensions have to become larger

in the future. The buckling strength of such large shells is influenced by many factors, among which are uncertainties in the complex boundary conditions of the soil as well as shell imperfections. For shell structures in general, it was found that geometric imperfections reduce the buckling resistance significantly [1; 2]. However, the choice of an appropriate imperfection form for numerical buckling analysis is not trivial. Current normative regulations require the selection of the most unfavorable imperfection form. Subsequently, an infinite number of possible imperfection patterns must theoretically be considered. In civil engineering, it is common to apply imperfections based on the first linear buckling mode. In previous work on suction buckets, imperfection forms based on linear buckling modes [3; 4] or circumferential welds and collapse affine imperfections [5] were considered. The aforementioned studies revealed that the first linear buckling mode is not always the most detrimental imperfection form which consequently does not yield a conservative value for the lowest possible buckling resistance. Thus, multiple modes and amplitudes have to be considered and a large number of simulations has to be conducted. In comparison to linear buckling modes, circumferential welds and collapse affine imperfections proved to be not particularly deleterious.

In contrast to a deterministic lower bound design, the buckling load can also be determined by a probabilistic analysis, where the stochastic scatter of geometric imperfections is considered. Imperfection patterns and the associated amplitudes result from numerous manufacturing steps. The manufacturing deviations lead to out-of-roundness, fabrication-related dents and weld depressions, which usually occur in combination and often dissimilar to linear buckling modes. In literature, several approaches to describe measured surface imperfections can be found. A very common and traditional approach is a Fourier series representation, more precisely the so called 'half-wave cosine' representation. Besides its frequent application in aerospace engineering [6–10], it has also been applied to measurements of civil engineering structures [11–13]. Other approaches are spectral representation methods like the Karhunen-Loéve expansion [14; 15] or evolutionary power spectra [16]. All of the latter methods require a large measurement database to obtain the stochastic properties of the shell set.

Within this work, an approach to statistically model more realistic imperfections is developed, which is based on only one measurement and uses the Fourier series representation. This paper is structured as follows: First, the underlying imperfection measurement is introduced, then, normative requirements are described. The Fourier half-wave cosine representation is described and the stochastic modeling scheme is introduced. In the following, the finite element model is described. Then, the results of the probabilistic analysis are shown and the buckling pressure is evaluated for different levels of reliability. Finally, the benefits and limitations of this approach are analysed and conclusions drawn.

2. Imperfections

Imperfections are recognized as the most important factor contributing to discrepancies between theoretical and experimental buckling resistances. For steel shells, geometric imperfections are considered to be more influential than material imperfections such as residual stresses or inhomogenities. Geometric imperfections are characterized by form and amplitude.

2.1. Measured imperfection data

Data of imperfection measurements of buckets or large cylindrical shells in general is very scarce, and nearly all of the publications available are on storage vessels with significantly smaller wall thicknesses. The only data available for this study is a laser scan published by LeBlanc [3] and considers the 'Mobile Met Mast' which was constructed in Aalborg, Denmark, in 2008. The dimensions of the bucket foundation are $L = 6\,\mathrm{m}$, $r = 6\,\mathrm{m}$ and $t = 20\,\mathrm{mm}$, with a maximum measured imperfection amplitude of 112mm [3]. The largest imperfections are found near the

four weldings in meridional direction. The measured imperfection amplitudes are shown in Figure 1.

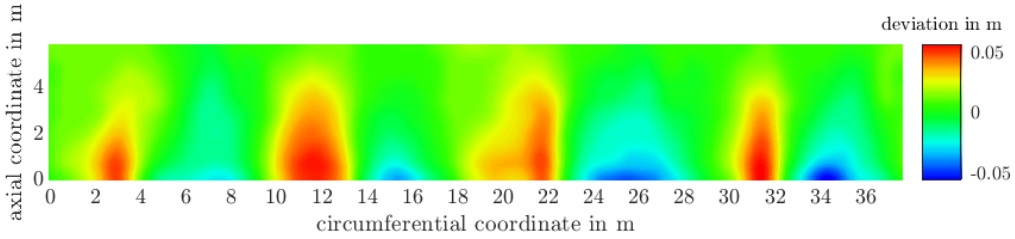

Figure 1. Measured imperfection according to LeBlanc[3]

2.2. Fourier representation of geometric imperfections

The measured out-of-plane geometric imperfection of shells can be treated as a two dimensional random field. Decomposing the imperfection into a truncated Fourier series proved to be an efficient way to describe measured geometric imperfections. Advantages are that the description of the imperfection does not depend on a fixed FE mesh with a certain fidelity and the data size is significantly reduced. One drawback is, that the classical formulation of the discrete two-dimensional Fourier series can only describe periodic functions. While the imperfection pattern of a cylinder is periodic in the circumferential direction, it is not in axial direction, where it generally has different imperfection amplitudes at the upper and lower edge of the cylinder. A very common way of dealing with this issue is to modify the Fourier series to yield the so-called 'half-wave cosine' approach, first introduced by Arbocz [6]. In the axial direction, a symmetry with $2L$ is assumed, which allows different imperfection amplitudes on the edges, and reduces deviations from the original function, compared to a periodic basis function. The half-wave cosine formulation is written as

$$\Delta w(x,y) = 2t \sum_{k=0}^{n_x} \sum_{l=0}^{n_y} \cos\left(\frac{k\pi x}{L}\right) \left(A_{kl} \cos\left(\frac{ly}{r}\right) + B_{kl} \sin\left(\frac{ly}{r}\right)\right) \tag{1}$$

where Δw is the out-of-plane deviation depending on the spatial coordinates x and y, $2L$ and $2\pi r$ are the periods in y and x direction. A_{kl} and B_{kl} are Fourier coefficients corresponding to k half waves in axial and l full waves in circumferential direction.

For this formulation, the Fourier coefficients of the measured geometric imperfection are determined by

$$A(k,l) = \frac{\alpha}{\pi L} \sum_{x=-L}^{L} \sum_{y=0}^{2\pi r} w_{real}(x,y) \cos\left(\frac{k\pi x}{L}\right) \cos\left(\frac{ly}{r}\right) \Delta x \Delta y \tag{2}$$

$$B(k,l) = \frac{\alpha}{\pi L} \sum_{x=-L}^{L} \sum_{y=0}^{2\pi r} w_{real}(x,y) \cos\left(\frac{k\pi x}{L}\right) \sin\left(\frac{ly}{r}\right) \Delta x \Delta y \tag{3}$$

where α is a numerical substitutor with $\alpha = 4$ for k or $l > 0$, $\alpha = 2$ for k and $l > 0$ and $\alpha = 1$ for k and $l = 0$. It is convention to normalize the Fourier coefficients by the shells' wall thickness, it is further possible to scale the measured imperfection amplitude according to the desired amplitude by scaling the Fourier coefficients. The Fourier coefficients of the bucket are shown in Figure 2, where the coefficients are particularly large for 4 ($l = 4$), 8 ($l = 8$) and 12 ($l = 12$) circumferential waves. These can be related to the number of welds.

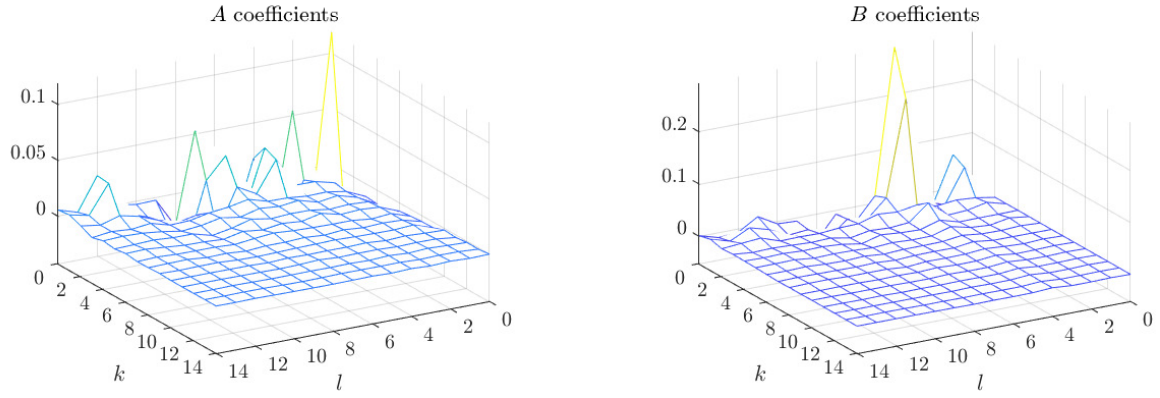

Figure 2. Fourier coefficients

2.3. Normative geometric imperfection requirements

In EN 1993-1-6, a distinction is made between deviations from the perfect shell which are measured to determine the quality of the shell and imperfections applied to the numerical models. For measured deviations, geometric tolerance requirements are given for out-of-roundness, unintended eccentricity and dimple tolerances, where weld depressions are included. Through dimension-dependent tolerance parameters for each imperfection category, shells are distinguished into three fabrication tolerance quality classes. For geometrically and materially nonlinear analyses with imperfections (GMNIA) of the shell, not all measured imperfection categories have to be applied. Instead, an equivalent geometric imperfection form should be applied, which has the most unfavorable effect on the buckling resistance. According to the requested fabrication tolerance class, the maximum geometric deviation of

$$\Delta w_{0,\mathrm{eq},1} = l_g U_n \tag{4}$$

$$\Delta w_{0,\mathrm{eq},2} = 25 t U_n \tag{5}$$

has to be applied, where l_g is the gauge-length which has to be individually determined for all significant stress situations, U_n is the dimple imperfection amplitude parameter depending on the tolerance class and t is the shell thickness. The definition of the required imperfection amplitudes refer to dimple imperfections. The dimple imperfection amplitude parameter differs for measured imperfection tolerances and the amplitudes applied to the numerical model. This difference is meant to cover all non-geometric imperfections, such as material inhomogeneities, variations in thickness, residual stresses, etc [2; 17].

The application of theses requirements poses some issues for suction buckets. The first question that arises is, whether the measured imperfection shape of four large waves at the skirt tip is categorized as dimple or out-of-roundness. Technically it cannot be counted to the dimple imperfections, since the imperfection waves are larger than the gauge length. In EN 1993-1-6, it is also not specified whether this form can be counted among the out-of-roundness imperfections, since the examples discussed in the Eurocode include only flattened or unsymmetrical shells. In the case of an even number of waves, the out-of-roundness measuring method of taking the largest distance across the shell is applicable. In contrast, in the case of an uneven number of waves, the resulting imperfection parameter is not comparable. In previous works, this imperfection type was however considered as an out-of-roundness deviation [4].

Similarly, when introducing imperfection forms on the numerical model, the choice of the amplitude is not trivial for both measured imperfections and buckling mode affine imperfections. The amplitude should be calculated according to the gauge length method, but the gauge length

is shorter than the waves. Recommendations or instructions for dealing with imperfections that do not have a dimple-like shape are not provided. For this work, the amplitude is defined as the distance of the outermost radial deviation to the innermost radial deviation, in agreement with previous work [4; 5]. The measured imperfection is scaled according to fabrication tolerance quality class C, which is the lowest quality class.

2.4. Stochastic modeling scheme

Since there is only one data set available from literature, it is challenging to extrapolate it to a stochastic sampling. The approach considered in this paper is based on a filtering technique which aims at maintaining the Fourier spectrum in an average sense. Another approach would be splitting the data into sectors and calculating statistical moments. The latter approach, however, enforces symmetries in the resulting imperfection fields, which is not desirable.

The imperfection measurements scaled to $\Delta w_{0,\mathrm{eq}}$ are decomposed into Fourier coefficients A_{meas} and B_{meas} according to Equation 2 and 3. The Fourier series is truncated to 15 coefficients as suggested by [18], shown in Figure 2. The coefficients are then used as a filter for white noise, as sketched in Figure 3. A two dimensional Gaussian white noise field is sampled and decomposed to Fourier coefficients with the same Equations 2 and 3 to yield A_{noise} and B_{noise}, which is then further processed to yield amplitude ξ_{noise} and phase terms.

$$\xi_{\mathrm{noise},k,l} = \sqrt{A^2_{\mathrm{noise},k,l} + B^2_{\mathrm{noise},k,l}} \tag{6}$$

The Fourier coefficients of the measurement are multiplied with the amplitudes of the white noise:

$$A_{\mathrm{sample},k,l} = A_{\mathrm{meas},k,l}\xi_{\mathrm{noise},k,l}n \tag{7}$$

and

$$B_{\mathrm{sample},k,l} = B_{\mathrm{meas},k,l}\xi_{\mathrm{noise},k,l}n \tag{8}$$

where the coefficients are scaled by a factor n to match the geometric deviation required by EN 1993-1-6. By maintaining the phases, the main characteristics such as the large imperfections at the skirt tips are transferred to all realizations. Figure 4 shows realizations of the dominating circumferential full wave B coefficients and the corresponding coefficients obtained from the measurement data.

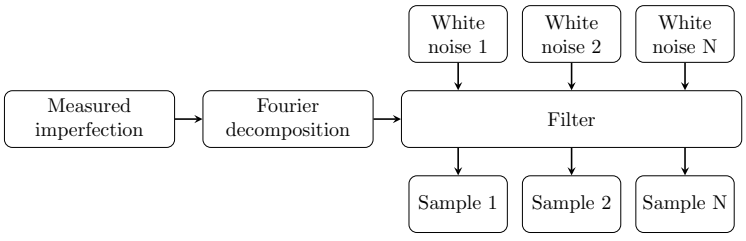

Figure 3. Stochastic modeling scheme

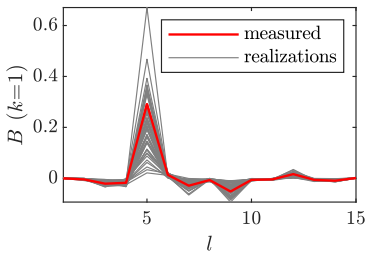

Figure 4. Coefficients of the realizations

3. Numerical Model

For the geometrically materially nonlinear analyses with imperfections (GMNIA), a finite element model is implemented in ABAQUS 2019. The bucket is modeled using quadrilateral shell

elements with reduced integration (S4R). A mesh of 52 axial elements and 176 circumferential elements is used, based on a previous convergence study. The material is structural steel S355 and it is modeled using a quad-linear stress-strain model according to Yun [19] considering an ultimate tensile strength of 490 MPa. For the finite element solver, it is converted to a true-stress/true-strain relationship.

The soil is modeled with C3D8R brick elements, implementing Mohr Coulomb plasticity, which is commonly used for describing sandy soils. For the presented simulations, a dense sand is assumed, with a Young's modulus of 50 MPa [3], a Poisson's ratio of 0.3, a density of 1000 kg m^{-3}, a friction angle of 38°, a dilatation angle of 8° and a lateral earth pressure coefficient of 0.5. The contact between the bucket skirt and the soil is modeled as Coulomb sliding, with an angle of friction of 24.7°. Initial geostatic stress considering the effective unit weight and the lateral earth pressure coefficient is introduced. In addition to the effective stress of the undisturbed soil, the stress resulting from the installation procedure is considered by applying the geotechnical model developed by Houlsby and Byrne [20]. Conservatively, a permeability ratio of 1.0 and a stress enhancement zone of 1.5 times the bucket diameter is assumed. The increase in vertical stress in the proximity of the bucket due to seepage and frictional forces leads also to a change of horizontal stress. These additional forces are superimposed to the applied internal negative pressure, which is constant on the skirt above the soil and on the lid. The negative pressure decreases from the mud-line to the skirt tip. The geometric imperfections are introduced as out-of-plane deviations to the suction bucket as well as to the adjacent soil nodes.

The analyses are conducted in a transient setting to assure numeric stability when solving for the contact problem. As the maximum pressure, the elastic buckling pressure of the ideal geometry is chosen. The imperfect elastic-plastic buckling resistance determined by a GMNIA is the lowest load obtained from the following three criteria, which are checked for when post-processing the simulations: maximum load factor of load-deformation curve, the bifurcation load factor, and the largest tolerable deformation given by EN 1993-1-6. For the combined circumferential and axial compression, a significant nonlinear effect can be noticed in the load deflection curve before the limit point of imperfect buckets is reached, compare Figure 5. Large buckles develop in the longitudinal direction as can be seen in Figure 6, around the larger inward buckles, small buckles to the outside develop, which stabilize the shell and in turn experience large stresses and plastification. The soil in contact with the shell also experiences plastic deformations which are caused by the out-of-plane movement of the shell skirt.

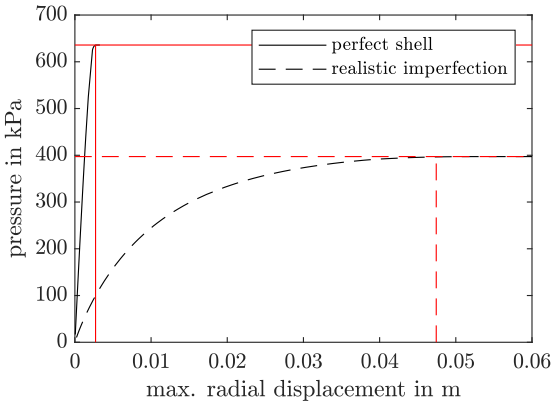

Figure 5. Pressure vs. radial displacement for perfect bucket and for bucket with large realistic imperfection

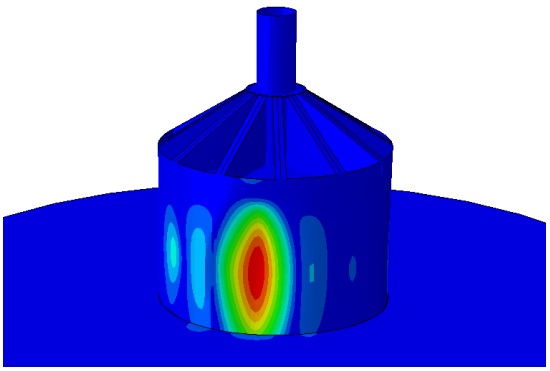

Figure 6. Deformation field of a shell with imperfections after reaching the maximum buckling pressure

4. Results

In the following, the resulting buckling pressures are analyzed regarding their distribution and evaluated for different reliability levels. Following the probabilistic analysis, the benefits and limitations of this method are discussed in detail.

4.1. Probabilistic analysis

The general aim of a probabilistic analysis is the determination of the cumulative distribution function F_λ of an objective function $\lambda(\mathbf{x})$ for a set of realizations $\mathbf{x}$. Here, the objective function $\lambda(\mathbf{x})$ is the buckling load which depends on the stochastically scattering imperfections. To determine the distribution of the buckling load, 500 realizations are generated, some examples are shown in Figure 7. The imperfections are introduced on the FE mesh and the GMNIA analysis is carried out for each realization. In all cases, a definite buckling limit load was obtained. Figure 8 shows the histogram of the buckling pressures. These are normally distributed, which agrees with findings from Kriegesmann [9]. The mean is $\mu_\lambda = 411\,\text{kPa}$ and the coefficient of variation is $c_{V,\lambda} = 0.0807$. To ensure that sufficient samples are evaluated, the convergence of the mean value and standard deviation are checked, see Figure 9.

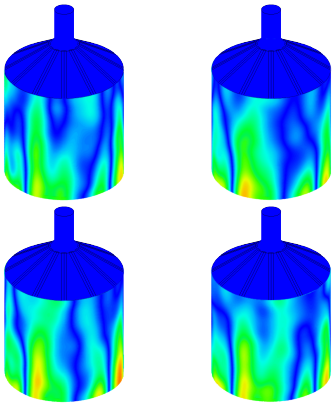

Figure 7. Realizations of the geometric imperfections

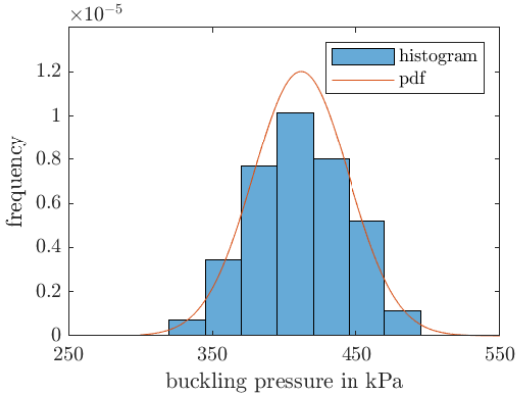

Figure 8. Probability density function of the buckling pressures for stochastic imperfections

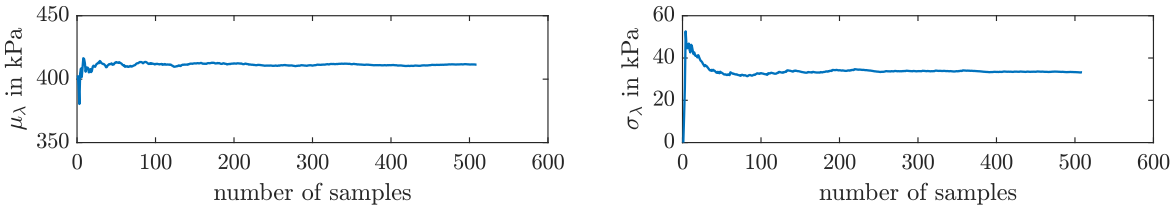

Figure 9. Convergence of mean value (left) and standard deviation (right) of the buckling pressure

4.2. Reliability-based buckling pressure

A probabilistic design pressure can be calculated from the reliability function, which is the complement of the cumulative distribution function. For the calculation of the reliability function $R(\lambda) = 1 - F(\lambda)$, the cumulative distribution function (CDF) $F(\lambda)$ belonging to the probability

density function is required. Therefore, the results shown in Figure 8 were transformed to the CDF shown in Figure 10. The probabilistic design value can be obtained by choosing a reliability level. With the mean μ_λ and standard deviation σ_λ, belonging to the CDF of the buckling loads, the distribution function can be evaluated for the chosen reliability level b. This results in a probabilistic design pressure λ_d

$$\lambda_d = \mu_\lambda - b\sigma_\lambda \tag{9}$$

where the factor b represents the chosen level of reliability and depends on the distribution type. For normal distributions, b equals the reliability index β, which is the number of standard deviations that separate the design value from the mean value. In EN 1990-1-1, a value of 3.8 is recommended for β, which equals a reliability of 99.99 %. The buckling strength distribution resulting from the stochastic approach can be evaluated regarding different levels of reliability, for example for a reliability of 99.9 % ($\beta = 3.09$) or 99% ($\beta = 2.33$) as shown in Figure 10. As a comparison, the buckling strength calculated using the stress-based method given in the Eurocode as well as the ideal elastic buckling strength are shown. As expected, the stochastic distribution fits between these extremes.

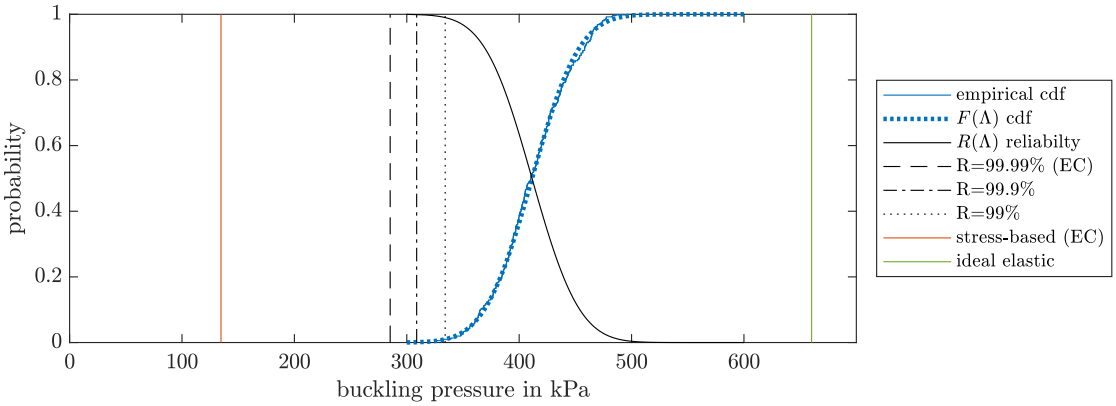

Figure 10. Evaluation for different reliability levels

4.3. Benefits and limitations

The major benefit of the half-wave cosine representation is the simplicity of application and the low number of Fourier coefficients that are needed to capture the main features of the imperfection pattern. However, a major shortcoming is the inability to describe non-zero gradients at the edges of the shell. This does not only lead to deviations from the original function at the shell edges, it also decreases the overall accuracy with increasing number of Fourier coefficients. An exemplary case is shown in Figure 11, where unphysical waves can be seen for the higher number of Fourier coefficients at the upper shell edge.

While this did not severely impact the early applications of the method with less than 16 coefficients, it becomes more problematic when aiming for a higher resolution. This issue can be minimized by mirroring the shell in axial direction and applying a full Fourier transformation. While the gradient will remain zero, the resolution can be significantly improved with longer Fourier series, see Figure 12.

Another subject worth considering is the treatment of spatial non-stationarity. The measured imperfection shows larger deviations from the perfect shell at the lower, free edge and smaller deviations at the edge welded to the lid. This might be a coincidence, but more likely it is due to the fabrication process. In order to draw a reliable conclusion, further measurement data would

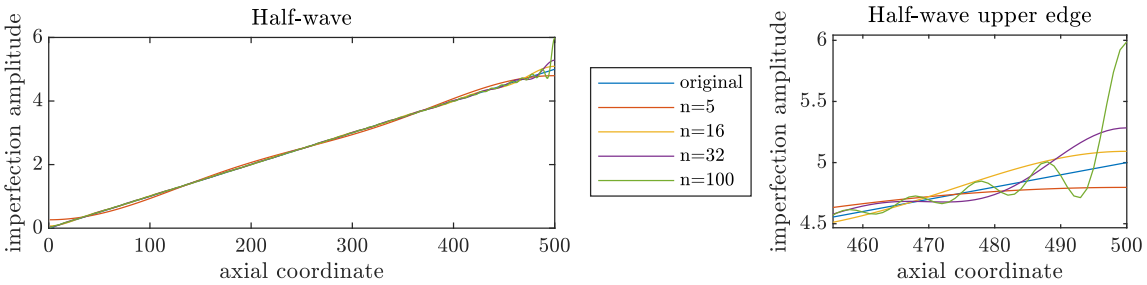

Figure 11. One-dimensional example of the half-wave cosine formulation considering different numbers of coefficients.

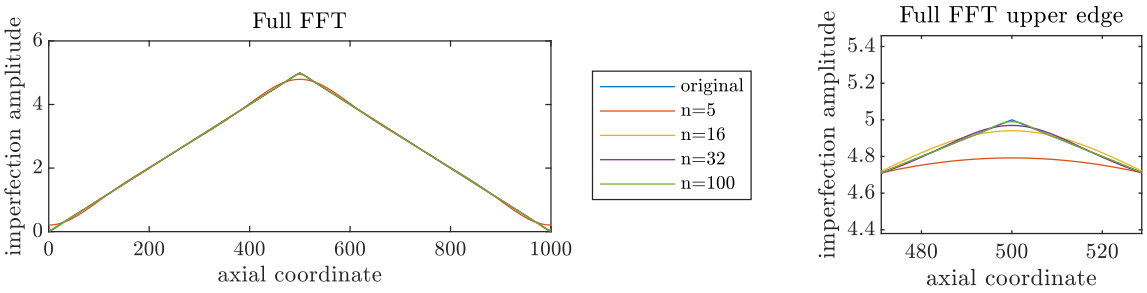

Figure 12. One-dimensional example of the mirrored Fourier formulation considering different numbers of coefficients.

be necessary. As mentioned in subsection 2.4, by varying only amplitudes within the 'half-wave cosine' approach, the larger imperfections of the realizations are predominantly at the lower edge. The deviation in axial direction is described only by cosine terms with half a cosine wave. By keeping the phase constant, the progression of the imperfection amplitude is transferred in the axial direction and no phase shifts in circumferential direction occur. Figure 13 shows the expected value and variance of the imperfection amplitude of all realizations. The imperfection fields are non-stationary, and the expected value reflects clearly the main characteristics of the measured imperfection. However, the high variance at the upper edge is not desired and can be attributed to the pure cosine formulation, where all coefficients lead to non-zero deviations at the shell edges. This could also be solved by using a full Fourier transform. A better approach to realize non-stationary fields could be to decompose the random field into a stationary part and a part accounting for the spatial evolution. The spatial part can be described by a homogeneous Fourier spectrum, multiplied by the spatial evolution. This idea is known as evolutionary power spectrum, methods to separate spectrum and spatial envelope can also be found in the literature [16; 21].

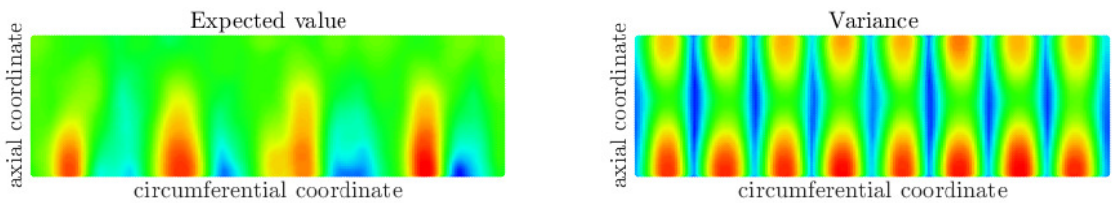

Figure 13. Expected value (left) and variance (right) of the generated imperfections

Regarding stochastic modeling of imperfections, the assumption is made that each

imperfection field is a realization of the manufacturing process, which is assumed to be a stochastic process governed by noise. Such an assumption is necessary, since distribution functions cannot be reasonably quantified from a single measurement. This essentially means that the generated realizations have similar spectral characteristics. For a large database of measurements, it would be considerably better to quantify statistical moments of Fourier coefficients and use these as a basis.

5. Conclusion and Outlook

This work presents a basic approach to model stochastic geometric imperfections of suction buckets in order to determine a probabilistic design pressure. As shown in Figure 10, the probabilistic evaluation of stochastic imperfection forms shows significantly less conservative results than the stress-based design with reduction factors. Compared to using buckling mode affine imperfections for GMNIA, the computational effort is not significantly higher, since this might require as much as 21 mode shapes [4], each evaluated for 10 amplitudes or more. With a Fourier representation, it is possible to model imperfections in a more realistic way, despite the limitations listed in subsection 4.3 and thus determine more realistic buckling pressures. It should be noted, however, that a safe probabilistic design must cover all relevant imperfections. Regarding the geometric imperfections, a wide data base would be desirable in order to identify stochastic properties of a shell series, which are influenced by the specific manufacturing and fabrication process. That would also enable the application of more sophisticated approaches, such as e.g. Karhunen-Loéve expansion or evolutionary power spectra. Possibilities for the implementation of such approaches despite a small data base will be subject of future research. Further, future work should consider more types of imperfections, since these also influence buckling pressures. Scattering of wall thicknesses, residual stresses from welding and scattering material stiffness for example could be taken into account within the probabilistic analysis. Finally, the stochastic modeling approach has to be validated with experimental data, which is also planned within the ProBucket project. In general, the application of probabilistic design approaches has a high potential for designing safer and more economic suction buckets. It can minimize the uncertainties in the assessment of the buckling strength and form a basis for reliable and robust prediction of the buckling pressure. Thus, the findings from this work can contribute to optimizing the design and form a basis for future work.

Acknowledgments

The work presented in this contribution was carried out within the joint project ProBucket. The authors kindly acknowledge the financial support provided by the German Federal Ministry of Economic Affairs and Climate Action (FKZ 03EE3033B). The technical support provided by the project partners is also gratefully acknowledged.

References

[1] Teng J G, Rotter J M, Teng J G and Rotter J M 2004 *Buckling of thin metal shells* (London: Spon Press;) ISBN 0419241906

[2] Rotter J M and Schmidt H 2013 *Buckling of steel shells : European design recommendations, ECCS* vol no. 125 (Rotterdam: ECCS - European Convention for Constructional Steelwork) ISBN 9789291471164

[3] Bakmar C 2009 *Design of Offshore Wind Turbine Support Structures: Selected topics in the field of geotechnical engineering* Ph.D. thesis Denmark

[4] Madsen S, Andersen L and Ibsen L 2013 *Engineering Structures* **57** 443–452 ISSN 0141-0296

[5] Gottschalk M 2017 *Zur Beultragfähigkeit von Suction Buckets* Doctoral thesis Leibniz University Hannover

[6] Arbocz J and Williams J G 1977 *AIAA Journal* **15** 949–956

[7] Elishakoff I and Arbocz J 1985 *Journal of Applied Mechanics* **52** 122 – 128 ISSN 0021-8936

[8] Hilburger M W, Nemeth M P and Starnes J H 2006 *AIAA Journal* **44** 654–663

[9] Kriegesmann B, Rolfes R, Hühne C, Teßmer J and Arbocz J 2010 *International Journal of Structural Stability and Dynamics* **10** 623–644

[10] Wagner H, Hühne C and Elishakoff I 2020 *Thin-Walled Structures* **146** 106451 ISSN 0263-8231

[11] Ding X, Coleman R and Rotter J M 1996 *Journal of Surveying Engineering* **122** 14–25

[12] Teng J, Lin X, Michael Rotter J and Ding X 2005 *Engineering Structures* **27** 938–950 ISSN 0141-0296

[13] Sadowski A J, Van Es S H, Reinke T, Michael Rotter J, (Nol) Gresnigt A and Ummenhofer T 2015 *Engineering Structures* **85** 234–248 ISSN 0141-0296

[14] Schenk C and Schuëller G 2003 *International Journal of Non-Linear Mechanics* **38** 1119–1132 ISSN 0020-7462

[15] Fina M, Weber P and Wagner W D 2019 *Proceedings of the 29th European Safety and Reliability Conference (ESREL)*

[16] Broggi M and Schuëller G 2011 *Engineering Structures* **33** 1796–1806 ISSN 0141-0296

[17] Ummenhofer T and Knödel P 1996 *Proc., Imperfections in Metal Silos–Measurement, Characterisation and Strength Analysis* 103–118

[18] Arbocz J and Abramovich H 1979 *The initial imperfection data bank at the Delft University of Technology: Part I*

[19] Yun X and Gardner L 2017 *Journal of Constructional Steel Research* **133** 36–46 ISSN 0143-974X

[20] Houlsby G T and Byrne B W 2005 *Geotechnical engineering* **158** 135–144

[21] Schillinger D and Papadopoulos V 2010 *Computer Methods in Applied Mechanics and Engineering* **199** 947–960 ISSN 0374-2830